

Petrochronology and petrogeochemistry of the Tamulangou Formation in Tahe area, northern Da Hinggan Mountains NE China: Geological implication

Shaoshan Shi^{1, a}, Shan Jiang^{1, b,*}, Yan Zhao^{1, c}, Yuan Yao^{1, d},
Yanqing Zang^{1, e}, Huiming Yu^{1, f}, Jihuan Wu^{1, g}, Xuguang Li^{1, h}, Yuli Wang^{1, i}

¹ Shenyang Center of Geological Survey, China Geological Survey, Shenyang, Liaoning, China.

^a geoshishaoshan@qq.com, ^{b,*} jiangshan1003@126.com, ^c zhaoyan_8@163.com,

^d 80806757@qq.com, ^e zangyanqing1989@126.com, ^f huiming2008@126.com,

^g wujihuan97@163.com, ^h john2011@163.com, ⁱ 329148612@qq.com

Abstract. This study reports petrography, petrogeochemistry and geochronology of Tamulangou Formation, which are located in Tahe, northern Da Hinggan Mountains, northeast China. In this study, we discussed their formation ages, petrogenesis, and tectonic environment. Zircon U-Pb dating results suggest formation ages of 148.1 ± 1.95 Ma and 161.5 ± 1.9 Ma for the conglomerate gravel, and the basaltic andesite, respectively. The geochemical characteristics indicate that the volcanic rocks in Tamulangou Formation are high-K calc-alkaline-shoshonitic rock that formed in a continental intraplate environment. All volcanic rocks of Tamulangou Formation in the study area are enriched in large ion lithophile elements and light rare earth elements and depleted in high field strength elements and heavy rare earth element. Combined with geochemical characteristics of the volcanic rocks and previous studies on the region, we concluded that the magma source of the volcanic rocks in the Tamulangou Formation derived from the enriched lithospheric mantle formed by metasomatism of subduction fluids. Comprehensive study suggested that the volcanic rocks from Tamulangou Formation in Tahe region all formed in a tectonic environment of lithospheric extension triggered by post-orogenic extension after the closure of the Mongol-Okhotsk Ocean.

Keywords: Da Hinggan Mountains; Petrogeochemistry; Tamulangou; Zircon U-Pb dating.

1. Introduction

The Da Hinggan Mountains (DHM) are located in a region of strong superposition, compounding, and transformation in the Paleozoic Paleo-Asian Ocean (PAO) tectonic domain, Mesozoic circum-Pacific tectonic domain, and Mongol-Okhotsk (MO) tectonic domain. Overall, its tectonic evolution is complex.

From the late Paleozoic to Early Mesozoic, the DHM experienced the closure of the PAO and MO oceans as well as the collision of multiple blocks [1]. The DHM entered a post-orogenic stage in the Late Mesozoic, with active volcanic eruptions and complex basin-ridge structures [2]. The Mesozoic volcanic rocks are widely exposed, and the rock types are complex. They are an important part of the Mesozoic igneous belt in eastern China and the margin of the Asian continent.

In recent years, many studies have been conducted on the formation age, geochemical characteristics, and tectonic setting of volcanic rocks in the DHM; however, the petrogenesis and tectonic setting of the Mesozoic volcanic rocks remain controversial [3-14]. These controversies are as follows: (1) whether the formation of Mesozoic volcanic rocks is either related to the rise of the deep mantle thermal plume resulting from the PAO closure [15-16] or due to the intraplate mechanisms [17]. (2) Whether these volcanic rocks are related to the subduction of the Paleo-Pacific plate [18-19] or the evolution of the MO ocean [20-22].

These discrepancies are caused by two gaps in research. First, the age of formation of the Mesozoic volcanic rocks in the DHM is uncertain. Second, the characteristics of volcanic geochemical evolution over time remain unclear, which also leads to uncertainties about tectonic

setting, rock genesis, and the dynamic nature of the formation. These limitations have hindered further research in this area.

On conducting a detailed study on the chronology of Mesozoic igneous rocks in eastern China, Wu et al. [23] attributed the large-scale magmatism to the subduction of the Pacific Plate. However, only few references to Mesozoic volcanic rocks widely distributed in the DHM are present, particularly due to the lack of accurate chronological data. Therefore, determining the formation age of the Mesozoic volcanic rocks in the DHM is crucial for an in-depth understanding of the age and genetic mechanisms of large-scale Mesozoic magmatism in the area. Furthermore, determining the age of the volcanic rock formation is helpful to explain the tectonic evolution and geodynamic process during the Mesozoic in eastern China. In addition, the key to ascertaining the formation age of the Mesozoic volcanic rocks in the DHM is to determine the initiation age and duration of volcanism.

At present, the consensus is that the Tamulangou Formation is the earliest volcanic stratigraphic unit in the DHM and comprises a set of basic volcanic rocks [24-25]. Therefore, determining the age of the volcanic rocks in the Tamulangou Formation is the key to determining the beginning of Mesozoic volcanism in the DHM. However, there is no consensus regarding the age division of the Tamulangou Formation. Most researchers believe that the basic volcanic rocks in the Tamulangou Formation formed during the Late Jurassic, but some believe that the formation age is Middle–Late Jurassic or even earlier. Therefore, determining the age of the Tamulangou Formation is of great significance for dividing and correlating Mesozoic volcanic strata in the DHM and to establish the chronological framework of Mesozoic volcanic rocks in the DHM.

In this study, by determining the geochronology and geochemical characteristics of the rocks of the Tamulangou Formation in Tahe in the northern section of the DHM, the authors discuss the age, petrogenetic environment, and tectonic setting of the formation. This study provides an important theoretical basis for the establishment of the geochronological framework of Mesozoic volcanic rocks in the DHM, and it is of great significance for an in-depth understanding of the genetic mechanism of large-scale Mesozoic magmatism in this area.

2. Regional geological setting

The DHM is situated in the eastern part of the Xingmeng Orogenic Belt, which is divided into the Erguna, Xing'an, and Songnen Blocks from north to south (Fig.1a). Since the Late Paleozoic, this area has experienced complex tectonic domain transformation. After the PAO closure, the Pacific tectonic domain gradually comprised the main portion of the area, thereby inheriting and gradually changing the original tectonic patterns of the PAO domain. The transformation process and the characteristics of multi-block and multi-stage evolution in the DHM [26] have created major challenges in gaining in understanding of the geological evolution process during the Late Paleozoic to Mesozoic.

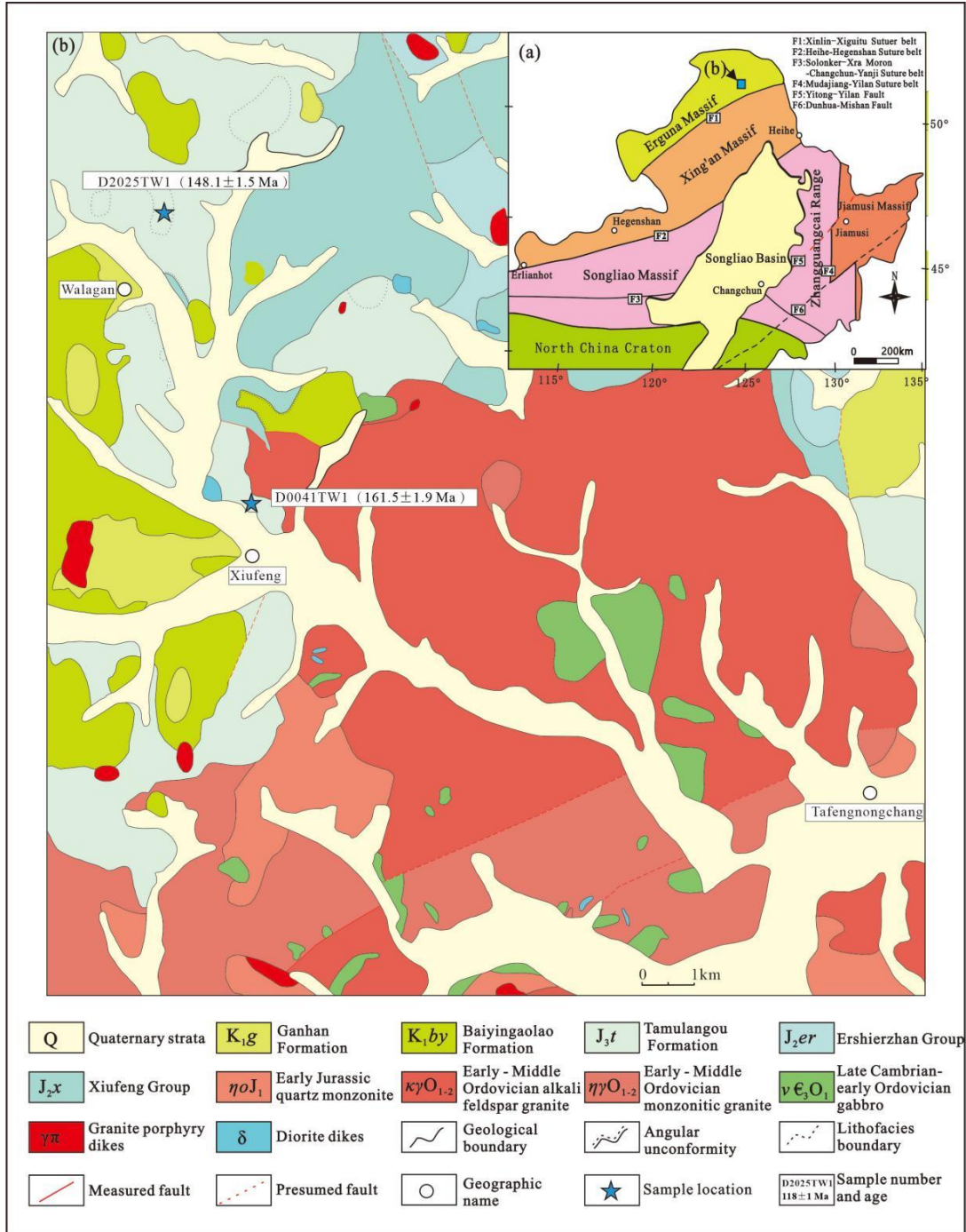


Fig. 1 Regional location map (a, after Wu et al. [26]) and Geological sketch map (b)

In the northern DHM, few pre-Cambrian crystalline basement rocks are exposed, including the Xinghuadukou and Jiahe Groups with amphibolite and greenschist phase transitions, respectively. The main lithology is a regional metamorphic rock series composed of plagioclase amphibolite, gneiss, schist, variolite, epigranulite, marble, and mixed rocks. The basement rocks in the area also contain a small number of Neoproterozoic granites; however, the distribution of these basement rocks is relatively limited.

The study area is in the Tahe region of the northern section of the DHM, which is located in the Erguna Block. The meso-Cenozoic tectonics are located in the DHM-superimposed orogenic system-rift and the DHM superimposed magmatic arc belt. Since the ancient Proterozoic, the DHM has experienced the formation of the continental basement (silica-aluminum crust), accretion and evolution of the PAO continental margin, and activity of the coastal Pacific continental margin. The basement is dominated by Late Cambrian–Early Ordovician granite with a few exposed basic

complexes. The overlying strata are mainly Mesozoic sedimentary and volcanic. From bottom to top, the sedimentary strata are the Xiufeng and Ershierzhan Formations, and the volcanic strata comprise the Tamulangou, Baiyingaolao, and Ganhe Formations (Fig.1b).

The Tamulangou Formation is mainly composed of volcanic lava with intermediate-basic spillage facies, most of which are grey green, grey purple, or grey black, with a stomatal almond structure developed and distinct rock flow characteristics, which mainly comprise basalt, trachyte basalt, olivine basalt, basaltic andesite, and some trachyandesite. The upper part of the Tamulangou Formation is predominantly sedimentary and is composed of fine conglomerate, medium-coarse conglomerate with volcanic breccia, and tuffaceous sandstone.

The conglomerate gravel lithology is basaltic andesite, with porphyritic texture and massive structures. The phenocrysts ($\pm 7\%$) are mainly composed of plagioclase and some amphibole. The predominant plagioclases are andesine ($>5\%$) with grain sizes $\leq 0.8 \times 1.2$ mm, and hornblende ($\pm 2\%$) with grain sizes $\leq 0.4 \times 1.0$ mm. The matrix ($\sim 93\%$) consisted of microcrystals and crystallites of plagioclase and amphibole with a small amount of microgranular black opaque iron minerals (Figure. 2a).

The basaltic andesite also has a porphyritic texture and a massive structure. Under the microscope, it shows a directional structure, which is indicated by the orientation trend of plagioclase and hornblende along the long axis and the matrix flow structure. The phenocrysts are mainly composed of plagioclase and amphibole. Plagioclase ($\pm 3\%$) is self-shaped plate columnar with particle size $\leq 0.5 \times 1.0$ mm. Hornblende ($\pm 2\%$) is self-shaped short columnar with particle size $\leq 0.4 \times 0.5$ mm. The matrix is a microcryptic structure composed of microcrystalline sperthite and hornblende and vitreous crystals (Fig.2b).

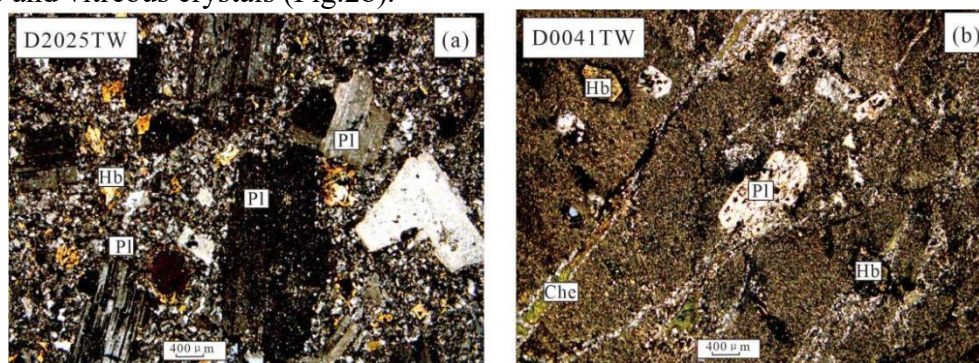


Fig. 2 Photomicrographs of the Tamulangou Formation of the study area. (a) Pebble of conglomerate; (b) Basaltic andesite. Q - quartz; Pl - plagioclase; Hb - hornblende; Che - chlorite

3. Analytical method

The sample crushing and zircon selection were completed by Langfang Yuneng Rock and Mineral Sorting Technical Service Co., LTD., Hebei Province.

Target preparation and obtaining images of cathodoluminescence (CL) and transmitted and reflected light and zircon U-Pb dating were completed at the State Key Laboratory of Continental Dynamics, Northwestern University. The Geo Las laser-ablation system was equipped with a 193 nm ArF excimer laser and an Agilent 7500a ICP-MS. Helium was used as a carrier gas to enhance the transport efficiency of the ablated material, Zircon 91500 was used as the external standard for age calculations, and NIST 610 silica glass was used as the external standard for concentration calculations. Measured U-Th-Pb isotope ratios were calculated using the CLITTER4.0 software. The weighted mean U-Pb ages and concordia plots were produced using the Isoplot program.

The analysis of major and trace elements was conducted with pollution-free equipment at the Northeast China Mineral Resources Supervision and Testing Center, Ministry of Natural Resources. The main process of testing and data processing and the main technical parameters of instruments are shown in Shi et al. [28].

4. Results

4.1 Zircon dating

Two rock dating samples, namely D2025TW and D0041TW, were collected from the conglomerate gravel above the Tamulangou Formation (124° 33 '57.1 "E, 52° 35' 51.6" N) and from the volcanic rocks of the Tamulangou Formation (124° 36 '53.3 "E, 52° 30'5.3"N), respectively. Colorless transparent zircons without inclusions and fractures were selected for U-Pb isotopic analysis. These zircons have high Th/U ratios of 0.18–1.09 (Table 1) and show distinct oscillatory zoning (Fig.3a, b), which is indicative of their typical magmatic origin [29]. The U-Pb dating results are listed in Table 1.

The zircons from the conglomerate gravel (D2025TW) were long and columnar, with lengths of 100–200 μm , showing typical magmatic zircon characteristics. Their length-width ratio was 1:2–1:4 (Fig.3a), and Th/U ratios were 0.18–0.75. Some zircons had narrow bright white edges, indicating weak recrystallization. U-Pb dating was conducted at 16 points, and we determined that the $^{206}\text{Pb}/^{238}\text{U}$ ages of these zircons were 146–149 Ma. The $^{206}\text{Pb}/^{238}\text{U}$ ages of these zircons were evenly distributed, yielding the weighted mean $^{206}\text{Pb}/^{238}\text{U}$ age of 148.1 ± 1.95 Ma (MSWD=0.072, n=16) (Fig.4a), which was interpreted to represent the crystallization age of the Tamulangou Formation.

The zircons of the basaltic andesite (D0041TW) were hemihedral long columns, with diameter axes ranging from 50 to 190 μm . The Th/U ratios were 0.38–1.09, and the length-width ratio was 1:1–1:3 (Fig.3b). The test results for the 21 valid points showed that the $^{206}\text{Pb}/^{238}\text{U}$ ages of these zircons ranged from 159 to 163 Ma. The $^{206}\text{Pb}/^{238}\text{U}$ ages of these zircons are evenly distributed, with a weighted average $^{206}\text{Pb}/^{238}\text{U}$ age of 161.5 ± 1.9 Ma (MSWD = 0.046, n=21) (Fig.4b), which was interpreted to indicate the crystallization age of Tamulangou Formation volcanic rocks.

4.2 Geochemical characteristics

The analysis results for major, trace, and rare earth elements (REEs) of Tamulangou Formation are listed in Table 2 (exclusive of loss on ignition).

Table 1. Zircon LA-ICP-MS U-Pb dating results for the Tamulangou Formation of the study area

Spot	Pb	Th	U	Th/U	Ratio				Age(Ma)			
	ppm				$^{206}\text{Pb}/^{238}\text{U}$	1 σ	$^{207}\text{Pb}/^{235}\text{U}$	1 σ	$^{206}\text{Pb}/^{238}\text{U}$	1 σ	$^{207}\text{Pb}/^{235}\text{U}$	1 σ
D2025TW												
2	1.66	30.19	66.76	0.45	0.02085	0.00052	0.14091	0.01006	148	3	149	9
4	2.71	53.08	107.16	0.50	0.02068	0.00049	0.14847	0.00811	147	3	156	7
5	2.18	38.91	88.52	0.44	0.02065	0.0005	0.13784	0.00817	147	3	146	7
7	2.40	45.3	88.55	0.51	0.02083	0.00051	0.14095	0.00871	146	3	149	8
12	2.28	41.06	86.64	0.47	0.02107	0.00049	0.13823	0.00778	149	3	146	7
13	2.11	37.39	78.55	0.48	0.02086	0.00054	0.1383	0.01003	148	3	147	9
14	2.16	61.2	81.68	0.75	0.02083	0.00062	0.13962	0.01453	148	4	148	13
16	2.30	36.4	89.03	0.41	0.02099	0.00054	0.14264	0.01057	149	3	150	9
17	3.0	73.	119.	0.61	0.02075	0.00051	0.1453	0.00885	147	3	153	8

	5	53	81									
19	2.7 7	52. 7	112. 89	0.47	0.02093	0.0005	0.1409 8	0.00799	148	3	149	7
20	3.6 0	54. 67	136. 4	0.40	0.02066	0.00048	0.1395 1	0.00699	147	3	148	6
21	2.3 9	48. 19	91.7 9	0.53	0.02099	0.0005	0.1375 3	0.00826	149	3	146	7
22	2.3 6	40. 3	83.8 5	0.48	0.02099	0.00051	0.1392 4	0.00886	149	3	147	8
23	6.9 4	53. 94	304	0.18	0.02082	0.00047	0.1421 8	0.00536	148	3	150	5
24	2.0 9	38. 15	78.0 4	0.49	0.02088	0.00049	0.1411	0.00764	148	3	149	7
25	1.6 2	26. 73	61.3 8	0.44	0.02100	0.00054	0.1317 4	0.01057	149	3	141	9
D0041T W												
1	3.4 4	89. 15	81.7 2	1.09	0.02943	0.00072	0.1988 0	0.01183	162	5	159	10
2	2.1 9	40. 31	51.4 6	0.78	0.02908	0.00075	0.1978 8	0.01833	160	5	158	16
3	3.0 8	73. 88	75.4 8	0.98	0.02927	0.00071	0.2061 4	0.01191	161	4	165	10
4	3.1 7	72. 29	72.4 2	1.00	0.02936	0.00070	0.2207 6	0.01058	162	4	178	9
6	2.3 2	47. 75	53.9 3	0.89	0.02928	0.00071	0.2047 9	0.01168	161	4	164	10
9	2.8 5	37. 86	69.1 2	0.55	0.02938	0.00081	0.2027 8	0.01668	162	5	162	14
11	2.6 6	48. 42	67.1 0	0.72	0.02932	0.00073	0.2139 5	0.01318	161	5	172	11
12	2.4 9	45. 76	59.8 8	0.76	0.02917	0.00075	0.1974 0	0.01865	160	5	158	16
13	3.1 7	57. 03	79.8 9	0.71	0.02932	0.00069	0.2132 6	0.01075	161	4	171	9
14	8.0 2	83. 47	220. 9	0.38	0.02964	0.00074	0.2045 8	0.01246	163	5	164	11
15	2.4 5	46. 57	60.5 9	0.77	0.02944	0.00069	0.2054 3	0.01055	162	4	165	9
16	1.8 0	31. 09	46.5 0	0.67	0.02942	0.00089	0.2150 9	0.02117	162	6	173	18
17	3.3 5	79. 03	77.6 0	1.02	0.02942	0.00071	0.2204 7	0.01172	162	4	177	10
18	3.1 2	70. 73	71.4 8	0.99	0.02964	0.00070	0.2042 9	0.01100	163	4	164	9
19	2.2 3	43. 93	52.6 1	0.84	0.02941	0.00075	0.2165 0	0.01468	162	5	174	12
20	2.0 4	39. 57	47.7 4	0.83	0.02951	0.00085	0.2005 8	0.01972	162	5	161	17
21	2.2 9	50. 33	55.5 5	0.91	0.02941	0.00070	0.1942 4	0.01117	162	4	155	9
22	2.7 1	55. 35	61.4 6	0.90	0.02943	0.00070	0.2045 1	0.01126	162	4	164	9

23	3.15	75.05	73.89	1.02	0.02931	0.00070	0.19900	0.01120	161	4	159	9
24	3.26	42.27	54.17	0.78	0.02904	0.00101	0.19950	0.02607	160	6	160	22
25	3.05	62.04	73.13	0.85	0.02898	0.00074	0.20465	0.02010	159	5	164	17

Table 2. Major (wt%) and trace ($\times 10^{-6}$) elements for the samples of the Tamulangou Formation

Sample	D0041	D0043	D0045	D0048	D2025	D0015GS1	D0016GS1	D0016GS2	D0048GS1	D6055GS1
SiO ₂	52.52	54.76	52.78	53.43	53.02	52.12	55.89	52.64	53.41	53.02
TiO ₂	1.04	1.01	1.03	1.06	1.05	1.01	1.02	1.03	1.07	1.05
Al ₂ O ₃	17.15	16.19	16.61	16.44	16.58	17.11	16.26	16.59	16.54	16.56
Fe ₂ O ₃	8.17	7.65	8.44	8.25	8.36	7.98	7.05	8.44	8.29	8.36
FeO	3.39	3.52	4.35	2.73	3.55	3.28	3.55	4.36	2.74	3.55
MnO	0.14	0.13	0.14	0.11	0.12	0.12	0.13	0.09	0.10	0.09
MgO	3.49	3.95	4.85	4.77	4.81	3.43	2.77	4.85	4.75	4.80
CaO	5.27	5.91	4.08	6.90	5.36	4.95	7.17	2.91	7.23	5.07
Na ₂ O	3.88	3.79	3.72	3.92	3.84	3.86	3.82	3.61	3.95	3.78
K ₂ O	3.85	2.37	2.69	2.03	2.43	3.82	2.33	2.67	1.97	2.32
P ₂ O ₅	0.32	0.30	0.33	0.28	0.31	0.29	0.30	0.33	0.28	0.30
LOI	0.78	0.42	0.97	0.15	0.57	4.96	3.03	6.65	2.15	4.40
A/NK	1.63	1.84	1.84	1.90	1.85	1.63	1.85	1.88	1.92	1.90
A/CNK	0.85	0.83	1.01	0.78	0.89	0.88	0.74	1.18	0.76	0.92
σ	6.05	3.17	4.03	3.35	3.81	5.97	2.94	3.75	3.36	3.55
TFeO	10.74	10.40	11.94	10.15	11.07	10.46	9.89	11.95	10.20	11.07
Mg#	24.52	27.52	28.88	31.96	30.29	24.69	21.87	28.86	31.77	30.24
K ₂ O/Na ₂ O	0.99	0.63	0.72	0.52	0.63	0.99	0.61	0.74	0.50	0.61
K ₂ O+Na ₂ O	7.73	6.16	6.41	5.95	6.27	7.68	6.15	6.28	5.92	6.10
Rb	60.82	51.96	72.29	32.42	52.44	60.84	51.93	72.25	32.47	52.40
Cr	17.92	58.83	64.24	134.55	99.38	17.90	58.88	64.22	134.53	99.37
Th	3.66	4.25	3.51	2.77	3.16	3.64	4.21	3.52	2.76	3.14
U	0.93	1.44	1.19	0.73	0.92	0.90	1.46	1.18	0.69	0.94
Li	17.16	6.52	29.97	3.78	16.86	17.17	6.51	29.95	3.73	16.84
Nb	6.94	8.22	8.88	6.56	7.62	6.96	8.20	8.81	6.53	7.67
Ta	3.11	0.73	1.02	0.69	0.89	4.17	0.75	1.03	0.68	0.86
Be	1.56	1.79	2.01	1.66	1.85	1.53	1.78	2.04	1.63	1.83
Ba	790.3	834.7	828.4	856.2	842.0	190.0	834.7	828.4	856.2	842.0
Sr	140.2	721.9	405.	121.4	217.1	110.0	921.9	415.7	100.0	217.0

			7							
Ni	39.53	46.09	45.2 5	64.91	62.09	9.55	47.07	45.16	74.90	60.03
Zr	145.2	166.7	174. 4	146.2	165.7	135.2	169.6	184.3	148.0	166.0
Hf	4.14	5.35	4.55	3.98	4.33	4.10	5.45	4.62	3.86	4.24
V	172.1	162.7	171. 3	157.7	165.7	172.1	142.8	172.5	148.6	160.0
Co	21.78	23.47	26.8 3	27.71	26.25	21.75	21.38	26.80	27.59	27.20
La	24.50	29.35	25.5 7	27.98	24.69	24.39	30.36	25.41	22.58	24.00
Ce	58.67	70.09	66.8 8	58.97	61.55	57.34	72.10	67.01	53.91	60.46
Pr	7.18	8.78	7.64	6.99	7.23	7.08	8.80	7.66	6.93	7.30
Nd	28.72	34.37	30.6 5	29.49	29.85	28.61	35.27	30.53	28.38	29.45
Sm	4.98	5.83	5.21	5.04	5.15	4.96	5.93	5.24	5.00	5.12
Eu	1.68	1.70	1.59	1.54	1.49	1.65	1.71	1.50	1.44	1.47
Gd	4.14	4.88	4.20	3.89	4.05	4.14	4.88	4.20	3.89	4.05
Tb	0.56	0.63	0.59	0.52	0.56	0.58	0.65	0.57	0.53	0.55
Continue Table 2.										
Dy	3.06	3.11	2.97	2.68	2.69	3.00	3.15	2.77	2.59	2.68
Ho	0.56	0.54	0.53	0.51	0.49	0.57	0.56	0.49	0.47	0.48
Er	1.56	1.51	1.37	1.35	1.28	1.57	1.50	1.27	1.26	1.27
Tm	0.24	0.23	0.21	0.19	0.21	0.26	0.24	0.20	0.19	0.20
Yb	1.57	1.50	1.35	1.32	1.32	1.66	1.52	1.20	1.20	1.20
Lu	0.24	0.23	0.16	0.18	0.17	0.25	0.21	0.17	0.17	0.17
Y	14.98	14.46	11.8 7	11.95	11.79	15.00	14.52	11.76	11.93	11.85
ΣREE	137.7	162.8	148. 9	140.7	140.7	136.1	166.9	148.2	128.5	138.4
LREE	125.7	150.1	137. 5	130.0	130.0	124.0	154.2	137.4	118.2	127.8
HREE	11.93	12.63	11.3 8	10.64	10.77	12.03	12.71	10.87	10.30	10.60
LREE /HRE E	10.54	11.89	12.0 9	12.22	12.07	10.31	12.13	12.64	11.48	12.06
La _N /Y b _N	11.19	14.04	13.5 9	15.20	13.42	10.54	14.33	15.19	13.50	14.35
δEu	1.13	0.97	1.04	1.06	1.00	1.11	0.97	0.98	1.00	0.99
δCe	1.08	1.07	1.17	1.03	1.13	1.07	1.08	1.18	1.06	1.12
Refere nce	This article					Reference[8]				

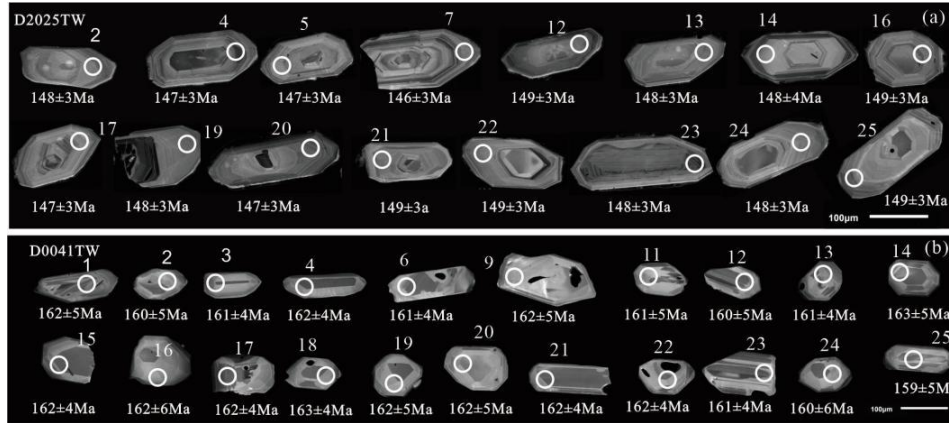


Fig. 3 Cathodoluminescence (CL) images of selected zircons from the Tamulangou Formation

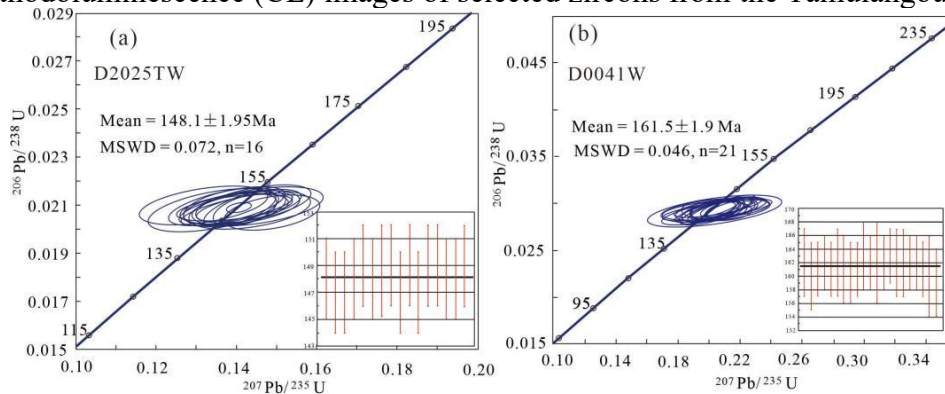


Fig. 4 Zircon U-Pb concordia diagram from the Tamulangou Formation of the study area

The samples of the Tamulangou Formation in Tahe are characterized by a variable content range of SiO₂ (52.12–55.89%), Al₂O₃ (16.19–17.15%), Na₂O+K₂O (5.95–7.73%) (Table 2), and MgO (2.27–4.85%). The magnesium index (Mg#) is 22–32. The K₂O/Na₂O ratios were 0.50–0.99, which is less than 1.

In the TAS diagram (that is, Total Alkali vs. Silica), majority of the sample lies in the alkaline series, and part of it falls near the dividing line between the alkaline and subalkaline series volcanic rocks. The overall lithology is basaltic trachyandean (Fig.5a), with a Rittman index (σ) of 2.49–6.05. In the SiO₂-K₂O diagram, the samples primarily belonged to the high-K-calc-alkaline shoshonite series (Fig.5b).

The Chondrite-normalized rare earth element (REE) patterns (Fig.6a) show that all the samples exhibit the same trend, with right-dipping characteristics of light REE (LREE) enrichment.

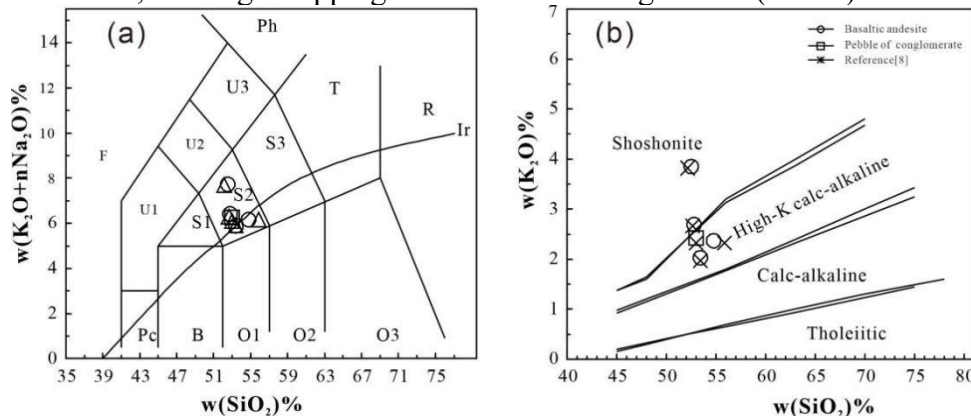


Fig. 5 SiO₂ vs. total alkali (Na₂O + K₂O) (a, after Le Maitre R. W. [30]) SiO₂ vs. K₂O (b, after Peccerillo and Taylor [31]) diagrams for the Tamulangou Formation of the study area.

Pc - Picrite basalt; B - basalt; O1 - Basalt-andesite; O2 - Andesite; O3 - Dacite; R - Rhyolit; S1-Trachybasalt; S2 - Basaltic trachyte andesite; S3 - trachyandensite; T - Trachyte\Trachy dacite; F-Feldspathoidite; U1-Tephrite\Basanite; U2-Phonotephrite; U3-Pollenite; Ph-phonolite; Ir-Irvine

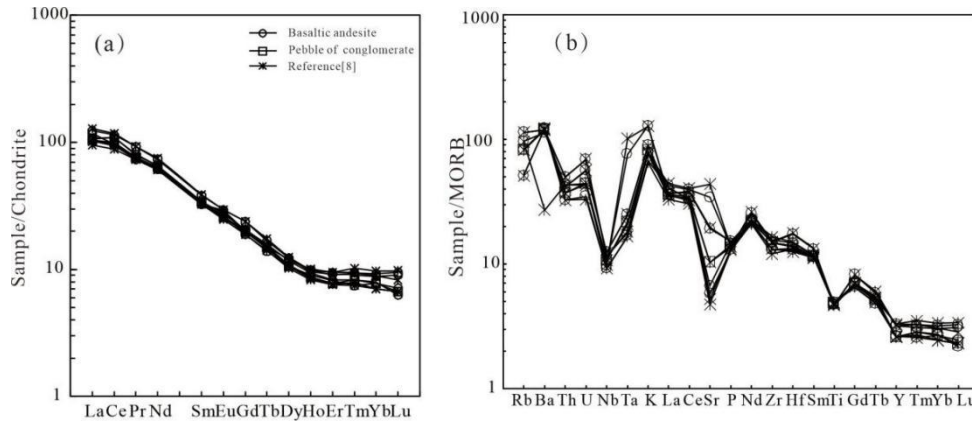


Fig. 6 Chondrite-normalized REE patterns (a, normalization values after Taylor and McLennan [32]) and Chondrite-normalized trace element spider diagrams (b, normalization values after Sun S.S. and McDonough W.F. [33]) for the Tamulangou Formation of the study area

The volcanic rocks of Tamulangou Formation in Tahe have high total REE ($\Sigma\text{REE}=128.54 \times 10^{-6} - 166.88 \times 10^{-6}$), notable fractional distillation of light and heavy rare earth elements, (La/Yb)_N values of 10.54–15.20, and a slight negative Eu anomaly ($\delta\text{Eu}=0.97 - 1.13$). This observation shows that the separation and crystallization of plagioclase are not predominant during the diagenetic process.

The chondrite-normalized trace element spider diagram (Fig.6b) shows that the samples are relatively enriched in large ion lithophile elements (LILEs; Rb, Ba, Sr, and K) and LREEs, and depleted in high field strength elements (HFSEs; Nb, P, Ta, Ti, and Yb).

The LILEs and LREEs suggest that the magma was derived from an enriched mantle source. The low HFSEs (Nb, Ta, and Ti) reveal the existence of fluid metasomatism in the magmatic source or the contamination of magma by crustal materials during the rise process.

The Chondrite-normalized trace element spider diagrams show an overall "uplift" feature, which is similar to the intraplate basalt distribution pattern [34]. The contents of incompatible elements Cr, Co, V, and Ni were $17.90 \times 10^{-6} - 134.55 \times 10^{-6}$, $21.38 \times 10^{-6} - 27.71 \times 10^{-6}$, $142.83 \times 10^{-6} - 172.49 \times 10^{-6}$, and $9.55 \times 10^{-6} - 74.90 \times 10^{-6}$, respectively. These trace element characteristics suggest that these rocks may be related to subduction metasomatism or crustal mixing.

5. Discussion

5.1 Age of formation

The formation age and stratigraphic division of the DHM Mesozoic volcanic rocks have always been debated among researchers. The division of volcanic strata in the DHM was mainly based on the correlation of rock assemblages and comparison of paleontological evidence. However, during the actual geological field study, the geological environment was determined as complex, vegetation coverage rate was high, and paleontological data were lacking. Therefore, the division of volcanic-sedimentary strata using the rock assemblage correlation method is erroneous. Therefore, accurate dating data are required to determine the attributes of the volcanic strata.

Recent studies on the geochronology of regional Mesozoic volcanic rocks indicate that the volcanic rocks of the Tamulangou Formation formed at 122 Ma [35], 138–129 Ma [36], 163–140 Ma (divided into two phases: 163–160 Ma and 147–140 Ma [37]), or 186–128 Ma (divided into four phases: 180 Ma, 165–160 Ma, 150–140 Ma, and 125 Ma [38]).

Zircon LA-ICP-MS U-Pb dating was conducted on conglomerate gravels and basaltic andesites from the Tamulangou Formation. The lithology of the gravel conglomerate is basaltic andesite (Fig.2a), and its composition is similar to that of the volcanic rocks in the Tamulangou Formation (Table 2). These characteristics are the same as those in Chondrite-normalized REE patterns (Fig.6a) and chondrite-normalized trace element spider diagrams (Fig.6b), indicating that the gravel

originates from the Tamulangou Formation, and is thus representative of its age. The zircon LA-ICP-MS U-Pb dating of the gravel and basaltic andesite distributed in Tahe region of the DHM revealed formation ages of 148.1 ± 1.95 Ma and 161.5 ± 1.9 Ma, respectively. According to the test results, the Tamulangou Formation in Tahe was deposited during Early–Late Jurassic or in the Late Jurassic (161–148 Ma).

5.2 Magma source

The volcanic rocks of the Tamulangou Formation in the Tahe region were enriched in LILEs and LREE and depleted in HREE and HSFEs, such as Nb, Ta, and Ti, indicating that the magma was contaminated by crustal materials during magma ascension or originated from enriched mantle melting.

The Nb/La vs. Ba/Rb diagram can distinguish between intercrustal and mantle origins [39], where the samples show a near-horizontal trend of subduction and enrichment (Fig.7a), indicating that the magma is uncontaminated or only slightly contaminated by crustal materials. This observation implies that the volcanic magma of the Tamulangou Formation in this area did not mix with crustal materials during its ascent. Therefore, the geochemical characteristics of the samples reflect the properties of the magma source region.

Therefore, the volcanic magma of Tamulangou Formation in the area was not obviously mixed with crustal materials during its ascent, and its geochemical characteristics mainly reflect the characteristics of its mantle source region.

The ratio of major elements K_2O/TiO_2 (1.84–3.78) and K_2O/P_2O_5 (7.04–13.17), and the ratio of trace elements La/Nb (2.87–4.26) and La/Sm (4.52–5.55) showed minimal change. These ratios indicate that crustal contamination had little influence on magmatic evolution [40]. Combined with the aforementioned geochemical characteristics, this finding suggests that the magma source region may have experienced metasomatism of the melt or fluid related to subduction after the exclusion of crustal mixing.

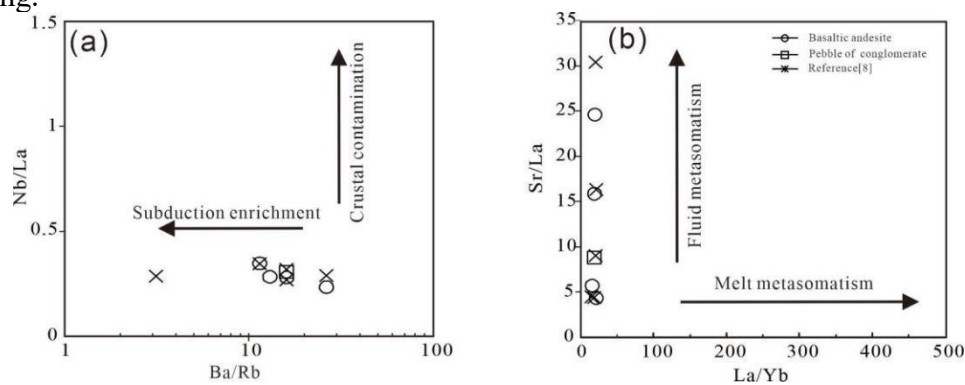


Fig. 7 Ba/Rb Vs. Nb/La (a) and La/Yb Vs. Sr/La (b) diagrams for the Tamulangou Formation

In conclusion, the volcanic rocks of the Tamulangou Formation in Tahe are enriched in LREE and LILEs, but depleted in HREE and HFSEs, which represent the geochemical characteristics of the magma melting source area. Because magmas from the enriched continental lithospheric mantle are usually deficient in HFSEs [41] and have high LILE/HFSE and LILE/LREE ratios, the contrary is true for magmas from the asthenospheric mantle.

In addition, a strongly incompatible element ratio is often used to reflect the source region characteristics because of its high stability during magmatic evolution, which is unaffected by separation crystallization or partial melting. The La/Nb ratio of basalts from the asthenosphere is less than 1.5 [42], and they have a relatively high TiO_2 content [43], whereas the La/Nb ratio of lava originating from or influenced by the lithospheric mantle is greater than 1.5 [44], and the TiO_2 content is relatively low. The samples of the Tamulangou Formation in the study area plot in the high-K calc-alkaline series on the K_2O vs. SiO_2 diagram (Fig.5b).

Previous studies have shown that potassium-high-K rocks mainly originate from the enriched mantle, with the addition of water and LILEs from subduction zones [45-46]. Subduction-related

metasomatism is the main mechanism of lithospheric mantle enrichment and consists mainly of fluid metasomatism formed by the dehydration of oceanic crust or melt metasomatism of oceanic crust sediments. The presence of subduction fluid and sedimentary melt metasomatism can be determined by the ratio of trace elements. Fluid-active elements, such as Ba, Rb, and Sr, easily migrate in the water-bearing fluid, whereas melt-active elements, such as Th and La, easily enter the sediment melt. Therefore, the ratio of the active elements of the fluid or sedimentary melt to the weakly active elements of the HFSES or HREE can be a good indicator of the contribution of subduction fluid and sedimentary melt to the mantle source region. For example, the linear trends of Ba/La and Sr/La indicate that fluids released from the subducted plate play a vital role, and those of La/Yb and Ce/Yb are due to the participation of subducted sediments in magmatism [47].

In the Sr/La vs. La/Yb and Ba/La vs. Ce/Yb diagrams (Fig.7b and 8a), the samples of the Tamulangou Formation in Tahe show a good subduction fluid metasomatism trend, which indicates that the fluid from the plate was added to the basalt mantle source, whereas the melt from the partial melting of the subducted sediments showed minimal effect. In addition, the samples had high Th/Zr and low Nb/Zr values (Fig.8b), indicating the dominance of subduction fluid metasomatism in the mantle [48]. Therefore, the volcanic magma of the Tamulangou Formation originated from lithospheric mantle metasomatized by subduction fluids.

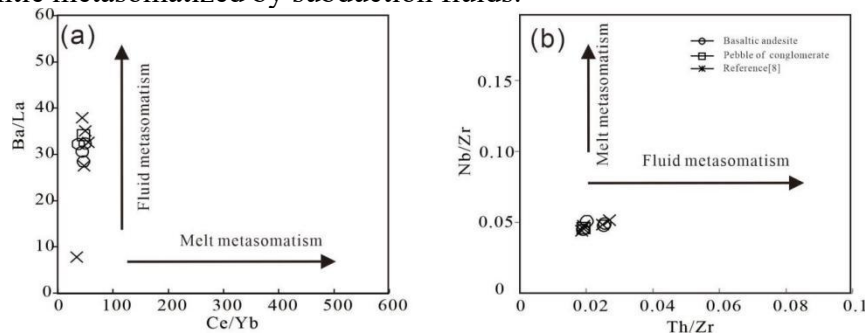


Fig. 8 Ce/Yb Vs. Ba/La (a) and Th/Zr Vs. Nb/Zr (b) diagrams for the Tamulangou Formation

5.3 Tectonic setting

In Th/Yb vs. Ta/Yb diagrams, the samples from the Tamulangou Formation in the study area plot in the volcanic rocks of the active continental margin (Fig.9a). Considering that the magma source area underwent subduction fluid metasomatism, continental basalts can be misjudged as island arc basalts.

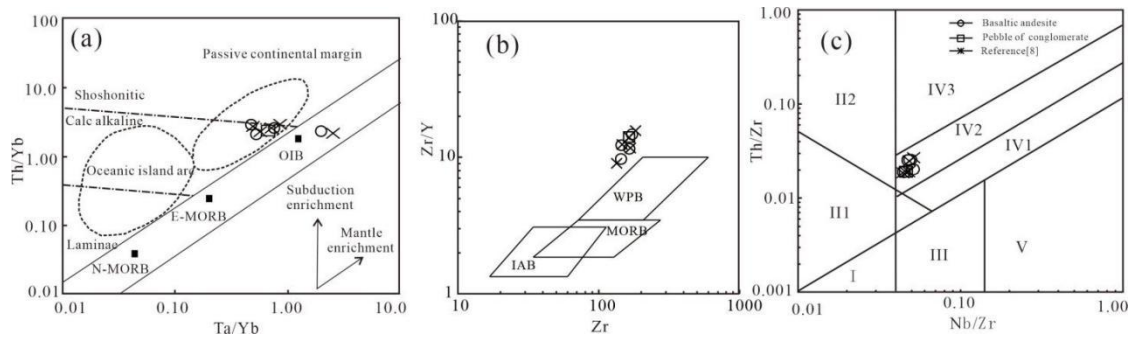


Fig. 9 Ta/Yb Vs. Th/Yb (a), Zr Vs. Zr/Y(b) and Nb/Zr Vs. Th/Zr(c) diagrams for the Tamulangou Formation of the study area

I - margin of divergent t oceanic plate; II - margin of convergent plate (II1 - island arc of continental margin; II2 - volcanic arc of continental margin; III - oceanic intra (the oceanic island and seamount, T - MORB, E - MORB); IV - continental intraplate (IV1 - continental rift; IV2 - tentional zone; IV3 - collision zone of two continental plate); V - mantle plume.

For basic lavas with subduction zone information, the use of Zr content, Zr/Y ratio, and Zr vs. Zr/Y diagrams can effectively distinguish continental basalts from island arc basalts [49]. The samples have high Zr content ($135.22 - 84.28 \times 10^{-6}$) and Zr/Y ratio (9.01 - 15.67). The samples

plotted in or near the intraplate basalts on the Zr vs. Zr/Y diagram (Fig.9b) indicated that they belonged to continental intraplate basalts rather than continental margin arc basalts. In addition, the Th/Zr vs. Nb/Zr diagram (Fig.9c) shows that the volcanic rocks of the Tamulangou Formation are intracontinental basalts that are located in the continental tensile zone (or initial rift) within the continental plate.

Three different views are present on the tectonic setting of the DHM Mesozoic volcanic rocks. Some scholars believe that the formation of Mesozoic volcanic rocks in this area is related to the subduction of the Paleo-Pacific Plate [21, 50], whereas others believe that it is related to the MO ocean evolution [10, 21, 51]. Some even believe that it is a result of a mantle plume [51].

The volcanic rocks of the Tamulangou Formation in the Tahe area formed in an intraplate environment and originated from the lithospheric mantle metasomatized by subduction fluids. Geophysical data show that the subduction of the Pacific Plate toward East Asia began in the Late Jurassic [52]; therefore, the dynamic source of metasomatic fluid and volcanic rock formation cannot be associated with the subduction of the Pacific Plate. The subduction fluid may have originated from remnants of the PAO or from the MO oceanic crust. The following evidence reinforces this view: (1) Late Jurassic volcanic rocks in Northeast China are mainly distributed in the DHM, at the south of the MO suture zone, and volcanism during this period was almost absent in the Songliao Basin and eastern Jihei [53]. In addition, the Paleo-Pacific Plate subducted northward toward Eurasia during this period [54], and the spatiotemporal characteristics of the volcanic rocks indicate that the formation of Late Jurassic volcanic rocks in the DHM was mainly related to the evolution of the MO ocean. (2) The formation age of the basalts in this area is approximately 100 Ma younger the final closure of the PAO [55], which is inconsistent with recent mantle metasomatism (which occurred shortly before partial melting) that was revealed by the decoupling phenomenon of high incompatible element enrichment and relative depletion of isotopic compositions. (3) The subduction of the Pacific Plate toward East Asia began in the late Jurassic [56]. (4) In terms of the formation age, the volcanic rocks far from the MO ocean showed a new trend in formation age [9, 57]

Regionally, the Mesozoic igneous rocks in the Jurassic Erguna Block are primarily composed of calc-alkaline igneous rocks, alkaline volcanic rocks developed in the Late Jurassic [58-59], and bimodal volcanic rocks developed in the Early Cretaceous. The change in magmatism features record the transition of the MO ocean from Early Jurassic oceanic subduction to Late Jurassic post-orogenic extension.

The study of Late Mesozoic igneous rocks in the Erguna Block shows that these granites are majorly A-type and A2-type [59], which were formed in the post-collision stretching stage of the MO ocean. Furthermore, the igneous rocks in this period tended to change from adakite to normal igneous rocks, indicating that the depth of the source rocks formed by partial melting during extension and collapse of the MO orogenic belt and crustal thinning became gradually shallower.

In conclusion, the magmatism of Tamulangou Formation is unrelated to the Pacific Rim tectonic system, and the regional dynamics are derived from the tectonic evolution of the MO tectonic belt. Therefore, the formation of volcanic rocks in the Tamulangou Formation is likely related to the tectonic environment of the lithospheric extension triggered by post-orogenic extension after the MO ocean closure and the metasomatic fluids originating from the MO subducted oceanic crust.

6. Summary

(1) Zircon U-Pb dating results show that the Tamulangou Formation in the Tahe area were formed in the late Jurassic (161.5 ± 1.90 Ma- 148.1 ± 1.95 Ma).

(2) The volcanic rocks of Tamulangou Formation in study area are enriched in LILEs and LREE, and depleted in HFSEs. The magma source region is an enriched lithospheric mantle with subduction fluid metasomatic.

(3) The formation of the volcanic rocks should be related to the postorogenic lithospheric

extension environment of the MO ocean after the collision and closure, and have no relationship with the Pacific Rim tectonic system. The regional dynamics are derived from the tectonic evolution of the MO tectonic belt.

Acknowledgements

Thanks to Wiley Editing Services for English language editing of this manuscript. We gratefully acknowledge the staff of the Northeast China Mineral Resources Supervision and Testing Center, Ministry of Natural Resources, the State Key Laboratory of Continental Dynamics, Northwestern University, Langfang Yuneng Rock and Mineral Sorting Technical Service Co., LTD., Hebei Province., and the Key Laboratory of Mineral Resources Evaluation in Northeast Asia for analysis of the samples. This study was supported by a scientific research grant from the National Natural Science Foundation of China (No. 42272253), the Geological Survey Project of China (No. DD20230437) and the Shenyang Science and Technology Talent Project (No. RC220450)

References

- [1] Zhao Xixi and Coe R.S. Paleomagnetic constraints on the paleogeography of China: Implications for Gondwanaland. *Abstract of 30th IGC*, 1996, 1(1): 231.
- [2] Li Sitian, Yang Sigong. The late Mesozoic rifting in the northeastern China and the fault-rifting basins in East Asia. *Science in China (Series B)*, 1987, 21(2): 185-195.
- [3] Lin Qiang, Ge Wenchun, Cao Lin, et al. Geochemistry of Mesozoic volcanic rocks in Da Hinggan Ling: the bimodal volcanic rocks. *Geochimica*, 2003, 32(3): 208-222.
- [4] Fan Weiming, Guo Feng, Wang Yuejun, Lin Ge. Late Mesozoic calc-alkaline volcanism of post-orogenic extension in the northern Da Hinggan Mountains, Northeastern China. *Volcano. Geotherm. Res.*, 2003, 121: 115-135.
- [5] Gao Xiaofeng, Guo Feng, Fan Weiming, et al. Origin of late Mesozoic intermediate-felsic volcanic rocks from the northern Da Hinggan Mountain, NE China. *Acta Petrologica Sinica*, 2005, 21(3): 737-748.
- [6] Fan Weiming, Guo Feng, Gao Xiaofeng, Li Chaowen. Sr-Nd isotope mapping of Mesozoic igneous rocks in NE China: Constraints on tectonic framework and crustal growth. *Geochimica*, 2008, 37(4): 361-372.
- [7] Li Zhumin, Shi Shaoshan, Li Yuhua, et al. Zircon U-Pb dating and geochemistry of the volcanic rocks of Tamulangou Formation in the south edge of Mohe Basin: Geological implication. *Geology and Resources*, 2015, 24 (06): 526-531.
- [8] Li, X.G.; Xue, C.J.; Wei, S.Y. Geochemical Characteristics and Tectonic Setting of Volcanic Rocks in Tamulangou Formation from Xinbaerhuyouqi Area, Inner Mongolia. *Uranium Geology*, 2021, 7(02): 216-226. (In Chinese)
- [9] Yang Huaben, Wang Wendong, Yan Yongsheng, et al. Origin of Basalts of the Tamulangou Formation and Mantle Enrichment in Xinlin Area, Northern Greater Hinggan Mountains. *Geological Review*, 2016, 62 (06): 1471-1486.
- [10] Yang Naifeng and Yang Liting. Zircon U-Pb geochronology, petrogeochemistry and tectonic significance of volcanic rocks from Tamulangou Formation in western Huzhong, northern Great Xing'an Range. *Global Geology*, 2017, 36(02): 361-370.
- [11] Shang, Y.H.; Lu, S.; Yue, H.J.; Wu, X.T. Geochronology and geochemistry of Tamulangou Formation volcanic rocks in Genh area. *Journal of Heilongjiang University of Science & Technology*, 2019, 29(05): 533-539. (In Chinese)
- [12] Zhang, S.Y. Geochronology and geochemistry of volcanic rocks in Tamulangou Formation from New Barag Ringt Banner, Inner Mongolia. *Journal of Jilin University (Earth Science Edition)*, 2020, 50 (01): 129- 38. (In Chinese)

- [13] Cui, J.R.; Han, Z.B.; Chen, D.B.; Li, Y. Geochronology and geochemistry of the andesites from Tamulangou formation in Badaguan area, Inner Mongolia. *Geology and Resources*, 2021, 30(04): 414-424. (In Chinese)
- [14] Liu, T.; Ji, F.; Wang, W.D.; Wang, J.Y.; Zhao, X.D. Discovery of the early Jurassic volcanic rocks in Xinlin area of Northern Daxinganling Mountains: Geological Implication. *Geology and Resources*. 2022, 31(1): 1-12. (In Chinese)
- [15] Ge Wencun. Geochemical characteristics and geotectonic background of the volcanic rocks in Da Hinggan Mountain, NE China. Ph.D. Thesis, Changchun University of Science and Technology, Changchun, China, 1977.
- [16] Lin, Q.; Ge, W.C.; Cao, L.; Sun, D.Y.; Lim, K. Geochemistry of Mesozoic volcanic rocks in DaHinggan Ling: The bimodal volcanic rocks. *Geochimica*, 2003, 32(3): 208-222. (In Chinese)
- [17] Shao, J.A.; Zang, S.X.; Mou, B.L. Extensional tectonics and asthenospheric upwelling in the orogenic belt: A case study from Hinggan-Mongolia Orogenic belt. *Chinese Science Bulletin*, 1994, 39: 533-537.
- [18] Sun, D.Y.; Xu, W.L.; Zhou, Y. Forming mechanism of the Mesozoic volcanic rocks in Da Hinggan Mountain, NE China. *Bulletin of Mineralogy, Petrology and Geochemistry*, 1994, 12(3): 162-164. (In Chinese)
- [19] Zhang Jiheng. Chronology and geochemistry of the Mesozoic volcanic rocks in the Great Xing'an Range, Northeastern China. Ph.D. Thesis, China University of Geosciences, Wuhan, China, 2009.
- [20] Chen, Z.G.; Zhang, L.C.; Zhou, X.H.; Wan, B.; Ying, J.F.; Wang, F. Geochronology and geochemical characteristics of volcanic rocks section in Manzhouli Xinyouqi, Inner-Mongolia. *Acta Petrologica sinica*, 2006, 22 (12): 2971-2986. (In Chinese)
- [21] Zhang, L.C.; Chen, Z.G.; Zhou X.H.; Ying, J.F.; Wang, F.; Zhang, Y.T. Characteristics of eep sources and tectonic-magmatic evolution of the Early Cretaceous volcanic in Genhe area, Da-Hinggan Mountains; constraints of Sr-Nd-Pb-Hf isotopic geocheistries. *Acta Petrologica sinica*, 2007, 23 (11): 2823-2835. (In Chinese)
- [22] Xu, W.L.; Ge, W.C.; Pei, F.P.; Meng, E.; Yu, Y.; Yang, D.B. Geochronological framework and tectonic implication of Mesozoic volcanism in Northeast China. *Bulletin of Mineralogy, Petrology and Geochemistry*. 2008, 27(Sup.): 286-287. (In Chinese)
- [23] Wu, F.Y.; Lin, J.Q.; Wilde, S.A.; Zhang, X.O.; Yang, J.H. Nature of significance of the Early Cretaceous giant igneous event in eastern China. *Earth Planet Sci. Lett.*, 2005, 233: 103-119.
- [24] Inner Mongolia Bureau of Geology and Mineral Resources. *Regional Geology of Inner Mongolia*. Geological Publishing House, Beijing, China, 1991. (In Chinese)
- [25] Heilongjiang Bureau of Geology and Mineral Resources. *Regional Geology of Heilongjiang Province*. Geological Publishing House. Beijing, China, 1993. (In Chinese)
- [26] Sengör, A.M.C. Natal'in B.A.; Burtman. V.S. Evolution of the Altaid tectonic collage and Palaeozoic crustal growth in Eurasia. *Nature*, 1993, 364: 299-307.
- [27] Wu, F.Y.; Sun, D.Y.; Ge, W.C.; Zhang, Y.B., Grant, M.L.; Wilde, S.A. Jahn, B.M. Geochronology of the Phanerozoic granitoids in northeastern China. *Journal of Asian Earth Sciences*, 2011, 41(1): 1-30.
- [28] Shi Shaohan, Shi Yi, Zhang Chao, et al. Geochronology and geochemistry of the Triassic intrusive rocks in the Faku area, northern Liaoning, China: Constraints on the evolution of the Palaeo-Asian Ocean. *Geological Journal*, 2022, 57(4): 1658-1681.
- [29] Hoskin P.W.O. and Ireland T.R. Rare earth element chemistry of zircon and its use as a provenance indicator. *Geology*, 2000, 28(7): 627-630.
- [30] Le Maitre R.W. *A Classification of Igneous Rocks and Glossary of Terms*. Blackwell, Oxford, 1989.
- [31] Pearce J.A. and Norry M.J. Petrogenetic Implications of Ti, Zr, Y, and Nb Variations in Volcanic Rocks. *Contributions to Mineralogy and Petrology*, 1979, 69: 33-47.
- [32] Taylor S.R. and McLennan, S.M. *The continental crust: its composition and evolution*. Oxford: Blackwell, 1985.
- [33] Sun S.S., McDonough W.F. Chemical and isotopic systematics of oceanic basalts: Implications for mantle composition and processes. In: Saunders A D, Norry M J, eds. *Magmatism in the Ocean Basins*. Geological Society, London, Special Publications, 1989, 42: 313-345.

- [34] Li, X.H. A geochemical constrain on Proterozoic crust growth and evolution-cited south China as instance. Science Press, Beijing, China, 1999.
- [35] Wu, G.; Zhu, Q.; Li, Z.T.; Wang, X.J.; Wang, H.B.; Li, G.Y.; Pang, Q.B. Geochemical feature and $^{40}\text{Ar}/^{39}\text{Ar}$ dating of the Mesozoic volcanic rocks in the northern Great Xing'an Rang. Abstract of 2005 National Meeting of the Petrology and Geodynamics in China, 2005, 1: 127-130. (In Chinese)
- [36] Fan Weiming, Guo Feng, Wang Yuejun, Lin Ge. Late Mesozoic calc-alkaline volcanism of post-orogenic extension in the northern Da Hinggan Mountains, Northeastern China. *Volcano. Geotherm. Res.*, 2003, 121: 115-135.
- [37] Wang Fei, Zhou Xinhua, Zhang Lianchang, et al. Late Mesozoic volcanism in the Great Xing'an Range (NE China): Timing and implications for the dynamic setting of NE Asia. *Earth and Planetary Science Letters*, 2006, 251: 179-198.
- [38] Zhang Jiheng, Ge Wenchun, Wu Fuyuan, et al. Large-scale Early Cretaceous volcanic events in the northern Great Xing'an Range, Northeastern China. *Lithos*, 2008, 102: 138-157.
- [39] Goswami T.K. Subduction Related Magmatism: Constrains from the REE Pattern in the Lohit Batholith, Arunachal Pradesh, India. *Geosciences*, 2013, 3(4): 128-141.
- [40] Jin Ling, Yang Weihong, Yang Deming, et al. Geochronology and geological significance of andesites from Meiletu Formation in Keyouzhongqi, Inner Mongolia. *Global Geology*, 2014, 33 (1): 49-58. (In Chinese)
- [41] Downes H. Formation and modification of the shallow subcontinental lithospheric mantle: a review of geochemical evidence from ultramafic xenolith suites and tectonically emplaced ultramafic massifs of western and central Europe. *Journal of Petrology*, 2001, 42: 233-250.
- [42] Guo Hongyu, Sun Deyou, Sun Rujian, et al. Chronology and geochemistry of Mesozoic volcanic rocks from southeastern Mohe Basin. *Global Geology*, 2015, 34 (1): 55-66.
- [43] Ewart A., Milner S.C., Armstrong R.A., Duncan, A.R. Enderbake volcanism of the Goboboseb mountains and Messum igneous complex, Namibia, part I: Geochemical evidence of Early Cretaceous Tristan Plume melts and the role of crustal contamination in the Parana-Enderbake CFB. *Journal of Petrology*, 1998, 39 (2): 191 - 225.
- [44] Zhou Jincheng, Jiang Shaoyoun, Wang XiaoLei, et al. Petrogeochemistry studies of the Middle Jurassic basalts in southern China taking Fujian Fangkeng basalt as an example. *Science in China (Ser. D)*, 2005, 35 (10): 927 - 936.
- [45] Zhang Qi, Jian Ping, Liu Dunyi. Zircon SHRIM geochronology and its significance of volcanic rocks in Ningwu. *Science in China (Ser. D)*, 2003, 33(4): 309-314.
- [46] Jia Wenchen, Zhang Baolin, Shen Xiaoli, et al. Geochemical characteristics and genesis of Late Paleozoic volcanic rocks in Erdenetsagaan region of southeastern Mongolia. *Journal of Jilin University (Earth Science Edition)*, 2012, 42 (2): 243-256.
- [47] Deniz K., Kadioglu Y.K. Assimilation and Fractional Crystallization of Foid-Bearing Alkaline Rocks: Buzlukdag Intrusives, Central Anatolia, Turkey. *Turkish Journal of Earth Sciences*, 2016, 25: 341-366
- [48] Kepezhinskas P., McDermott F., Defant M.J., et al. Trace Element and Sr-Nb-Pb Isotopic Constraints on a Three-Component Model of Kamchatka Arc Petrogenesis. *Geochimica Acta*, 1997, 61(3): 577-600.
- [49] Xia Linqi, Xia Zuchun, Xu Xueyi, et al. The discrimination between continental basalt and island arc basalt based on geochemical method. *Acta Petrologica et Mineralogica*, 2007, 26(1): 77-89.
- [50] Chen Zhiguan, Zhang Lianchang, Zhou Xinhua, et al. Wang, F. Geochronology and geochemical characteristics of volcanic rocks section in Manzhouli Xinyouqi, Inner-Mongolia. *Acta Petrologica Sinica*, 2006, 22(12): 2971 - 2986.
- [51] Yang Naifeng, Yang Liting. Zircon U-Pb geochronology, petrogeochemistry and tectonic significance of volcanic rocks from Tamulangou Formation in western Huzhong, northern Great Xing'an Range. *Global Geology* 2017, 36(2), 361-370.
- [52] Richards M.S. Prospecting for Jurassic slabs. *Nature* 1999, 397: 203-204.
- [53] Xu Wenliang, Wang Feng, Pei Fuping, et al. Mesozoic tectonic regimes and regional ore-forming background in NE China: Constraints from spatial and temporal variations of Mesozoic volcanic rock associations. *Acta Petrologica Sinica*, 2013, 29(2): 339-353.

- [54] Safonova I.Y., Utsunomiya A., Kojima S., et al. Pacific superplume-related oceanic basalts hosted by accretionary complexes of central Asia, Russian Far East and Japan. *Gondwana Research*, 2009, 16(3/4), 587-608.
- [55] Sun Deyou, Wu Fuyuan, Zhang Yanbin, et al. The final closing time of the west Lamulun River-Changchun-Yanji plate suture zone: Evidence from the Dayushan granitic pluton, Jilin Province. *Journal of Jilin University (Earth Science Edition)* 2004, 34(2): 174-181.
- [56] Vander V.R., Spakman W., Bijwaard H. Mesozoic subducted slabs under Siberia. *Nature*, 1999, 397: 246-249.
- [57] Meng FanChao, Liu JianLin, Cui Yan, et al. Mesozoic tectonic regimes transition in the North east China: Constraints from temporal spatial distribution and associations of volcanic rocks. *Acta Petrologica Sinica* 2014, 30(12): 3569-3586. (In Chinese)
- [58] Zhao Zhonghua, Sun Deyou, Gou Jun, et al. Chronology and Geochemistry of volcanic rocks in Tamulangou Formation Southern Manchuria, Inner Mongolia. *Journal of Jilin University (Earth Science Edition)*, 2011, 41(6): 1865-1880.
- [59] Gou Jun, Sun Deyou and Qin Zhen. Late Jurassic-Early Cretaceous tectonic Evolution of the Great Xing'an Range: Geochronological and Geochemical evidence from granitoids and volcanic rocks in the Erguna block NE China. *International Geology Review* 2019, 61 (15-16): 1842-1863.